Available online at www.sciencedirect.com
SCIENCE DIRECT®
Earth and Planetary Science Letters 241 (2006) 466–476
EPSL
www.elsevier.com/locate/epsl

Os isotope heterogeneity of the upper mantle: Evidence from the Mayarí–Baracoa ophiolite belt in eastern Cuba

R. Frei [a,*], F. Gervilla [b], A. Meibom [c], J.A. Proenza [d], C.J. Garrido [b]

[a] *Geological Institute, University of Copenhagen, Øster Voldgade 10, DK-1350 Copenhagen, Denmark*
[b] *Departamento de Mineralogía y Petrología and Instituto Andaluz de Ciencias de la Tierra (Universidad de Granada-CSIC) Facultad de Ciencias, Avda. Fuentenueva s/n, 18002 Granada, Spain*
[c] *Muséum National d'Histoire Naturelle, Laboratoire d'Etude de la Matière Extraterrestre, USM 0205, Case Postale 52, 57 Rue Cuvier, 75005 Paris*
[d] *Departament de Cristallografia, Mineralogia i Dipòsits Minerals, Facultat de Geologia, Universitat de Barcelona, Martí i Franquès s/n, 08028, Barcelona, Spain*

Received 26 April 2005; received in revised form 31 October 2005; accepted 28 November 2005
Available online 4 January 2006
Editor: E. Boyle

Abstract

In an attempt to quantify the extent of geochemical heterogeneity within a restricted and well dated portion of the upper mantle, 27 chromite separates from the 90 My old chromite deposits in the Mayarí–Baracoa ophiolite belt in eastern Cuba have been investigated for platinum group element (PGE) concentrations and Re–Os isotopic systematics. The samples are characterized by systematically subchondritic initial $^{187}Os/^{188}Os$ ratios and substantial heterogeneity. The initial $^{187}Os/^{188}Os$ ratios vary with chromite chemistry and with geographical distribution, reflecting differences in the Os isotopic evolution for the different upper mantle sections represented by the ophiolite. Accordingly, the Os isotope data might be divided into three groups. In the Moa–Baracoa district, where the chromite bodies are located in the mantle–crust transition zone, the calculated initial γOs values average -0.97 ± 0.69 ($n=13$). In the Sagua de Tanamo district, where chromite chemistry is highly variable and their location in relation the mantle sequence is less clear, the initial γOs values are intermediate, with an average of -1.77 ± 0.80 ($n=7$). In the Mayarí district, where the chromite bodies are located in the lower part of the mantle sequence, initial γOs values average -2.66 ± 0.29 ($n=7$). These subchondritic (i.e. negative) initial γOs values are most simply explained by Re depletion during ancient partial melting and/or melt percolation events.

The Os isotope heterogeneity documented here indicates a high degree of geochemical complexity on small to intermediate length scales in the upper mantle. Our results, in combination with data on chromites from the literature, show that an "average present-day Os isotopic composition" for the hypothetical depleted MORB mantle (DMM) reservoir cannot be precisely established beyond the statement that it is "broadly chondritic". Indeed, the upper mantle cannot be considered a sufficiently homogeneous geochemical "reservoir" to serve meaningfully as a baseline against which geochemical "anomalies" are evaluated. On the other hand, our findings are consistent with the "Statistical Upper Mantle Assemblage" or "SUMA"-concept, according to which a high level of geochemical heterogeneity is maintained in the upper mantle at all relevant length scales, as a result of the plate-tectonic cycle and intra-mantle processes such as melt-migration and metasomatism.
© 2005 Elsevier B.V. All rights reserved.

Keywords: Os isotopes; chromite; ophiolite; SUMA; Cuba

* Corresponding author.
E-mail address: robertf@geol.ku.dk (R. Frei).

0012-821X/$ - see front matter © 2005 Elsevier B.V. All rights reserved.
doi:10.1016/j.epsl.2005.11.043

1. Introduction

Traditionally, mantle geochemistry has been based primarily on analyses of oceanic basalts [1]. Based on oceanic basalt geochemistry, including noble gas isotopic systematics and lithophile radiogenic isotopes, a number of geochemical endmembers have been defined: depleted MORB mantle (DMM), enriched mantle (EM1and EM2), high-μ (HIMU), focal zone (FOZO) etc. [1,2]. For decades, the underlying assumption in the geochemical literature has been that each of these reservoirs can be described by a set of well-defined isotopic and trace-element characteristics, and ascribed to different regions in the mantle with a distribution reflecting the large scale geophysical mantle structure. In this way, the DMM reservoir, the presumed homogeneous source of MORB, became synonymous with the convective upper mantle, extending down to the 660 km seismic discontinuity [3]. All other reservoirs have traditionally been placed in the lower mantle and major efforts have been directed towards understanding the processes that formed each different reservoir [1,2,4,5]. Radiogenic isotopes have played a very important role in this development and have provided information regarding the time-integrated geochemical evolution of each hypothetical reservoir. This has allowed models of large-scale geochemical differentiation and dynamic mantle evolution to be constructed, as summarized in [1].

While oceanic basalts have contributed enormously to our understanding of the geochemical evolution of the mantle and have provided a sense of the different geochemical "flavors" that are present in the mantle, there is one significant drawback. Oceanic basalts are derived from the upper mantle by partial melting, melt-migration, mixing and homogenization [6]. These processes obscure the true geochemical variability in the source material and its spatial distribution, and make it difficult to relate the geochemistry of the basalts at the surface to the structure and dynamics of the mantle below.

Fortunately, as a result of different tectonic environments and processes, relatively large pieces of oceanic crust and/or upper mantle sequences have been preserved along current and past subduction and suture zones. When a complete suite of crustal and mantle sequences can be observed, such bodies are referred to as ophiolites [7,8]. Ophiolites, or the simpler peridotite massifs, can represent large fragments of paleo-oceanic lithosphere that offer an opportunity to sample directly the type of depleted source material from which MORB is being extracted. A number of important upper mantle complexes have been the subject of systematic geochemical studies. Perhaps the best example is the Ronda peridotite massif in Spain. Here, large isotopic heterogeneities in $^{143}Nd/^{144}Nd$, $^{87}Sr/^{86}Sr$, $^{206}Pb/^{204}Pb$, and $^{187}Os/^{188}Os$ have been documented on a variety of length scales, ranging from centimeters to tens of kilometers. The now classical study by Reisberg and Zindler [9] on Ronda was among the first to direct attention towards the possible high degree of geochemical heterogeneity in the upper mantle, despite the observed (relative) homogeneity of MORB. The lesson from Ronda is clear: only direct sampling of upper mantle sequences will expose the true geochemical variability in the upper mantle and will allow the characteristic length scales and isotopic compositions of different upper mantle lithologies to be determined precisely.

Recently, several studies have focused on the understanding of heterogeneities in the convective upper mantle. In an attempt to determine the average $^{187}Os/^{188}Os$ of the hypothetical DMM reservoir, Walker et al. [10] presented Re–Os isotopic data of chromites separated from the upper mantle or lower crustal portions of 18 ophiolites ranging in age from 900 to 50 Ma. In contrast to previous studies that were conducted on bulk peridotites [11] and sulfides associated with MORB [12] and which provided ambiguous results (see e.g. [13]), the above study exclusively used chromite with well-constrained stratigraphic positions within the ultramafic sequences of the ophiolites sampled. Chromite has the advantage over silicates in that it is not strongly affected by serpentinization, which can lead to open-system behaviour of the Re–Os system [11,14,15]. In addition, chromite normally is characterized by very low Re–Os ratios and elevated Os concentrations, which makes age corrections to their the initial Os isotopic compositions and model ages relatively small. Büchl et al. [16] presented Re–Os isotopic analyses of ultramafic rocks from two mantle sections of the Troodos Ophiolite and showed that Os isotopic heterogeneities result either from Re depletion events during ancient partial melting and melt percolation (chondritic to subchondritic $^{187}Os/^{188}Os$ ratios) or from the addition of radiogenic Os during subsequent (low degree) melt percolation events (suprachondritic $^{187}Os/^{188}Os$ ratios). The overall spread in Os isotopic composition in both studied mantle sections from the Troodos crustal section ranges from 0.1169 to 0.154, and almost spans the entire range of $^{187}Os/^{188}Os$ ratios for the convecting mantle, defined by modern MORB glasses and sulfide inclusions [12,13], by chro-

mites in ophiolites of different ages [10], and by abyssal peridotites and chromite grains in abyssal peridotites [11,17]. From these considerations it becomes clear that there is a general problem in defining a meaningful average Os isotopic composition for any hypothetical upper mantle reservoir [18]. At least two factors might further contribute to this: (1) the addition of radiogenic Os by seawater contamination (but see [13]), and (2) the affinity of Os for trace phases such as sulfides, metal alloys [19] and chromites that, combined with its extremely low solubility in silicates and the relative inertness of these trace phases towards melting, can cause serious nugget effects; see e.g. [18]. Such considerations constitute a fundamental problem for the ongoing debate about the interpretation of mantle osmium isotopic systematics [10,11,20].

Here we present a study of Os-isotope and platinum group element (PGE) systematics of a suite of 27 chromite separates from the Mayarí–Baracoa Ophiolite Belt in eastern Cuba. The data are discussed in the context of intra-sample heterogeneity, ophiolite geology, and geochemical evolution of the upper mantle.

2. Geological background and samples

2.1. Geological relationships

The Mayarí–Baracoa Ophiolite Belt includes a set of allochthonous massifs of Upper Cretaceous age (~88–91 Ma [21]) and is a prominent geological feature extending along more than 1000 km in north-eastern Cuba (Fig. 1). In the easternmost part of this belt, the Moa–Baracoa massif and the Mayarí–Cristal massif crop out, and constitute the so-called "Mayarí–Baracoa belt" ([22]). These massifs extend over roughly similar areas, 1200 km^2 and 1500 km^2, respectively, but exhibit different lithospheric sections (Fig. 1).

The Moa–Baracoa massif is ca. 2.5 km thick and consists of a lower unit of mantle tectonites overlain by a crustal section ~500 m thick made up of layered gabbros, pillowed basalts and radiolarites. This sequence is, in some places, tectonically inverted with a volcano-sedimentary unit overthrust by gabbro and/or mantle ultramafics. Mantle tectonites are partly serpentinized, highly depleted (mostly free of clinopyroxene)

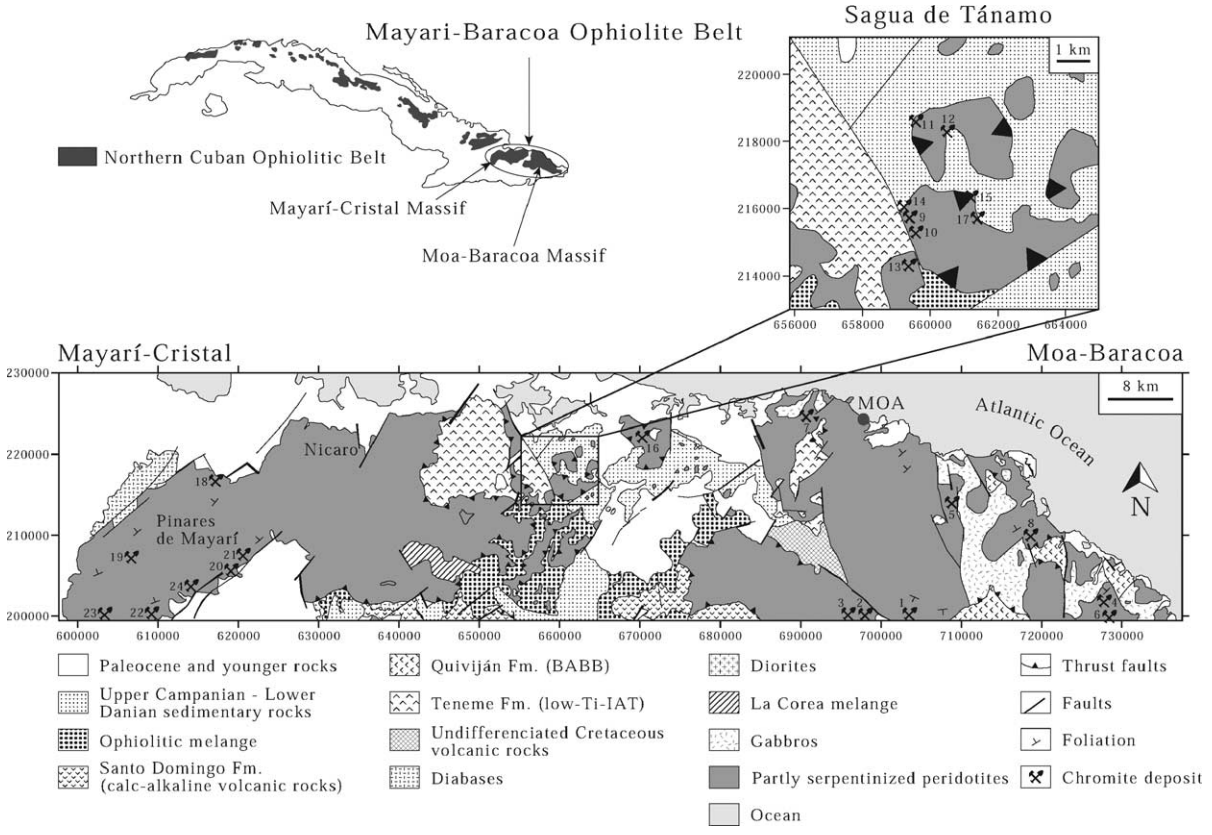

Fig. 1. Simplified geological map of the Mayarí–Baracoa ophiolite belt (Cuba). The locations of the three major mining districts Mayarí, Sagua de Tánamo and Moa–Baracoa are indicated. Numbers identifying chromite deposits from which samples are presented herein correspond to those listed in Table 1. Coordinates are UTM, based on the Caribbean grid system.

Table 1
Re and PGE concentrations, Cr numbers and Os isotopic data of chromites from the Mayari–Baracoa ophiolite belt, eastern Cuba

Sample	Mines	$^{187}Os/^{188}Os$	Δ (%)	Os (ppb)	Re (ppt)	$^{187}Re/^{188}Os$	T_{Ma} (Ma)	T_{RD} (Ma)	$^{187}Os/^{188}Os_i$	γOs	Cr#	Pd (ppb)	Ir (ppb)	Pt (ppb)	Pd/Ir
Moa–Baracoa district															
AM-4	Amores (4)	0.12584	−0.34	19.52	1176	00.2896	475	132	0.12540	−0.80	0.45	13.61	7.07	2.37	1.93
CG-8	Cayo Guam (5)	0.12737	−1.16	11.54	2092	0.8716	83	–	0.12606	−0.28	0.47	99.75	20.27	33.58	4.92
CG-9	Cayo Guam (5)	0.12495	−4.39	17.82	939	0.2534	717	265	0.12457	−1.46	0.52	78.60	12.82	6.31	6.13
G12-24	Mercedita (1)	0.12561	−1.26	9.13	940	0.4952	–	166	0.12487	1.22	0.45	10.26	4.88	9.69	2.10
G15-15	Mercedita (1)	0.12504	1.29	25.22	739	0.1409	386	251	0.12483	−1.25	0.45	12.96	10.09	6.23	1.28
G-15-19	Mercedita (1)	0.12497	−0.08	46.69	1120	0.1153	368	262	0.12479	−1.28	0.45	16.26	18.28	7.45	0.89
L2-1	Mercedita (1)	0.12532	−1.82	11.84	1433	0.5820	–	209	0.12445	−1.55	0.45	33.51	5.58	1.59	6.01
LN-2	LosNaranjos (6)	0.12593	0.04	15.70	451	0.1381	179	118	0.12573	−0.54	0.50	9.08	12.12	7.82	0.75
NS-4	Narcisco	0.12716	−0.17	7.42	1174	0.7605	73	–	0.12601	−0.31	0.49	9.31	5.75	6.44	1.62
PO-101	Potosi (8)	0.12420	–	16.91	665	0.1891	710	376	0.12392	−1.97	0.51	19.04	7.69	5.50	2.48
PO-104	Potosi (8)	0.12571	–	44.64	789	0.0850	192	151	0.12558	−0.66	0.57	13.21	14.99	6.70	0.88
PO-5	Potosi (8)	0.12603	–	3.48	917	1.2665	–	103	0.12413	−1.80	0.55	44.98	4.04	2.99	11.13
PO-7	Potosi (8)	0.12828	–	426.45	76655	0.8642	201	–	0.12698	0.45	0.55	281.45	173.87	16.37	1.62
Average									0.12518	−0.97	0.49				3.21
1σ									0.0008	0.69	0.04				3.04
Sagua de Tanamo district															
A3A	Albertina (13)	0.12573	−0.36	87.73	889	0.0487	168	148	0.12566	−0.60	0.69	11.74	25.50	4.54	0.46
C-ANT	Cernicalo (11)	0.12472	−1.19	12.25	658	0.2583	836	299	0.12433	−1.64	0.55	8.59	4.68	3.26	1.84
G-1	Guarina (17)	0.12487	0.18	40.59	1509	0.1787	497	276	0.12460	−1.43	0.71	21.62	13.60	24.05	1.59
MB-1	Monte Bueno (16)	0.12238	−1.29	1219.10	506	0.0020	650	647	0.12237	−3.19	0.69	15.25	47.51	16.94	0.32
NV-100	Negro Viejo (12)	0.12459	−0.14	53.29	951	0.0858	404	318	0.12446	−1.54	0.61	11.11	29.00	7.49	0.38
R-100	Rupertina II (10)	0.12374	−2.18	17.72	465	0.1262	648	444	0.12355	−2.26	0.52	10.14	7.79	3.19	1.30
TI-1	Tiberia (14)	0.12638	0.21	3.63	1072	1.4186	–	51	0.12425	−1.71	0.61	11.35	55.84	5.58	0.20
Average									0.12418	−1.77	0.63				0.87
1σ									0.00101	0.80	0.07				0.68
Mayari district															
CA-BB	Casimba (19)	0.12342	−2.02	9.22	591	0.3082	2102	492	0.12296	−2.73	0.74	12.64	25.80	8.75	0.49
CS-100	Casimba (19)	0.12319	−1.26	42.00	1414	0.1619	879	526	0.12295	−2.74	0.74	11.54	37.70	7.33	0.31
CS-2	Casimba (19)	0.12295	−0.05	117.64	1188	0.0486	639	562	0.12288	−2.79	0.74	13.55	39.58	7.34	0.34
EM-5	Estrella de Mayari (21)	0.12315	−0.60	56.59	719	0.0611	627	532	0.12306	−2.65	0.76	9.89	37.62	6.46	0.26
J-4	Juanita (22)	0.12358	−1.35	95.52	836	0.0421	523	468	0.12352	−2.29	0.75	12.17	18.87	6.09	0.64
J-5	Juanita (22)	0.12428	−0.77	11.55	1252	0.5210	–	364	0.12350	−2.30	0.75	7.92	37.95	3.08	0.21
V-3	Victoria (24)	0.12249	−0.46	245.57	590	0.0116	650	631	0.12247	−3.12	0.78	12.88	17.84	3.89	0.72
Average									0.12305	−2.66	0.75				0.43
1σ									0.00037	0.29	0.01				0.20

γOs (at 90 Ma) is calculated using the parameters from [50] and λ for $^{187}Re = 1.666 \times 10^{-11}$ a^{-1} [51]. Uncertainties are ±5% or better for Re and $^{187}Re/^{188}Os$, better than ±0.1% for Os and $^{187}Os/^{188}Os$, and better than 0.5% for calculated $^{187}Os/^{188}Os_i$ and γOs units.

Δ is the deviation (in %) of the measured $^{187}Os/^{188}$ Os ratio of chromites relative to the measured $^{187}Os/^{188}Os$ ratio of respective chromitite whole rock powders [27].

Numbers following the mine specifications correspond to those marked on Fig. 1.

Cr# represents average values of multiple electron microprobe spot analyses of chromite grains on the scale of a thin section [27].

harzburgites and minor dunites ([23]. At the mantle–crust transition zone, these ultramafic rocks become rich in plagioclase and clinopyroxene, and contain thick (up to 20 m) tabular gabbro bodies parallel to the foliation of the host peridotite and chromite deposits ([22]). Different generations of gabbro, pegmatitic gabbro and microgabbro dikes cut through all the rock types described above ([22,23]).

The Mayarí–Cristal massif shows a thick unit (>5 km) of partly serpentinized peridotites with tectonite structure, topped by few hundred meters of massive microgabbro. Peridotite consists of depleted (mostly free of clinopyroxene) harzburgite containing subconcordant, less than 1-m-thick dunite layers and chromitite bodies surrounded by dunite envelopes. Several generations of cross-cutting dikes of websterites (few centimeters to few tens of centimeters of thickness) cut through harzburgite, dunite and chromitite. In the upper part of the section, harzburgite too is cut by abundant micro-gabbro dikes up to 20 m thick. In the easternmost part of the massif (Sagua de Tánamo region) the peridotite slab becomes very thin (<1 km) and over-thrusts highly fractured mélanges consisting of different types of ophiolitic rocks mixed with arc-related volcanic and sedimentary rocks of Cretaceous age.

2.2. Chromite deposits

A total of 174 chromite deposits of variable size have been described from within the Mayarí–Baracoa belt ([24]). These deposits have been grouped into three mining districts [22], according to the composition of chromite ore: (1) the Moa–Baracoa district; (2) the Sagua de Tánamo district, and (3) the Mayarí district.

The *Moa–Baracoa* district comprises the whole Moa–Baracoa massif and has the largest chromite deposits of the region. All these deposits contain Al-rich chromite (Cr#=0.43–0.54, Table 1). The ore bodies have tabular to lenticular shapes, show variably thick dunite envelopes and are concordant with the foliation of the host peridotite. Most chromitites contain concordant, tabular bodies of gabbro, rare dunite layers and are cut by several generations of pegmatitic gabbro dikes ([22,25]). Chromite texture is mainly massive but some bodies show disseminated-, nodular- or anti-nodular-textured ores at their rims.

The *Sagua de Tánamo* district has a set of 35 small deposits located in the easternmost part of the Mayarí–Cristal massif ([22,26]). The chemistry of their chromite ore is highly variable, ranging in composition from Al-rich (Cr#=0.52) at Rupertina II, to Cr-rich (Cr#=0.71) at Guarina (Table 1). These deposits are concordant and subconcordant with the foliation of the enclosing peridotites and exhibit variably thick dunite envelopes. Primary chromite textures are typically massive, disseminated and banded.

The *Mayarí* district is located in the western part of the Mayarí–Cristal massif and includes medium- to small-sized deposits of chromite rich in Cr_2O_3 (Cr#>0.73; Table 1). Chromitite bodies are pod-like in shape, most of them are located deep in the mantle sequence of the massif and always occur concordant to the foliation of the host peridotite. They frequently exhibit a zoned structure showing massive chromitite in the center and either nodular or disseminated ore at the rims.

2.3. Samples

In this study, 27 purified chromite separates derived from chromite deposits located in the ultramafic portions of the Mayarí–Baracoa Ophiolite Belt were examined. In a companion study [27], Re–Os isotopic results from a subset of samples were performed on bulk chromitite with chromite contents of more than ~85 vol.%. The chromites analyzed herein were previously characterized by electron microprobe, and bulk chromitites were analyzed for platinum-group element (PGE) concentrations by ICP-MS and a few samples by INAA after nickel sulfide fire assay [27]. The study by Gervilla et al. [27] revealed that chromites from these chromitites are not chemically zoned. In addition, platinum-group minerals hosted by the chromitites (either contained as inclusions directly in chromite, or located in the silicate matrix of cataclastized chromite or within fractures of the latter) were identified and described in detail.

3. Analytical techniques

The chemical separation techniques used in this study for Re–Os analyses follow procedures described previously [28]. Briefly, the samples were dissolved and equilibrated with an ^{185}Re and ^{190}Os spike by "inversed" *aqua regia* digestion in sealed Carius tubes. 200–300 mg chromite (50–200 μm grain size), together with 6 ml of inversed *aqua regia* (1/3 concentrated HCl, 2/3 concentrated HNO_3) were frozen into the tubes, sealed and heated to 230 °C for 2 days. Osmium was extracted from the inversed *aqua regia* by distillation directly into 3 ml 8N HBr and purified by a microdistillation procedure adopted from [29]. Rhenium was purified by carbon-tetrachloride extraction according to the procedure of [30]. Total analytical

blanks averaged about 15 ± 6 pg for Re (with a natural composition of Re) and 9 ± 3 pg for Os (with $^{187}Os/^{188}Os$ ratios of 0.16 ± 0.02). All Os isotopic data reported here are blank corrected and respective blank uncertainties were propagated to the final isotopic and concentration determinations. The blank corrections were found to be negligible for the Os analyses, and minor for most Re analyses.

An aliquot of the sample solution after distillation was spiked with a mixed ^{191}Ir-^{110}Pd-^{194}Pt tracer to measure the respective concentrations of these elements by isotope dilution analysis, performed on a Perkin Elmer Elan 5000 quadrupole instrument at the Geological Survey of Denmark and Greenland. The counting errors of the respective isotopic masses were on the order of 2–5%, which translates to errors of the relevant ratios used for the concentrations of these elements of <~7%. The isotopic composition of Re was measured separately via solution ICP-MS on the same facility, whereby the solutions were doped with natural Ir for online mass bias control of the $^{185}Re/^{187}Re$ ratio via the ratio $^{191}Ir/^{194}Ir$. The external reproducibility for repeated analyses of standard solutions of comparable amounts is approximately ± 0.3% for Re.

Osmium isotopic analyses were performed on the VG Sector 54 solid-source negative thermal ionization mass spectrometer at the University of Copenhagen, using a multi-collector static routine. Analyses were accomplished using Faraday cups. $^{189}Os/^{188}Os = 1.21978$ was used for in-run fractionation corrections. Samples were loaded in 1.5 μl 8N HBr onto high purity Pt filaments and 0.5 μl of a saturated $Ba(OH)_2$ solution was added as an ionization activator and analyzed at temperatures >800 °C. Repeated analyses of 1 ng loads of the University of Maryland Johnson Matthey reference solution yielded an external reproducibility of ± 0.07% (2σ; $n = 15$) of the ratio $^{187}Os/^{188}Os = 0.11377$. Repeated multi-dynamic analyses of 50 ng loads of the University of Maryland Johnson Matthey reference solution using $^{189}Os/^{188}Os = 1.21978$ for in-run fractionation corrections yielded an external long-term precision of ± 50 ppm ($2\sigma_m$) of the ratio $^{187}Os/^{188}Os = 0.113789$; $n = 38$). Respective analyses in static multi-collection mode yielded corresponding external precisions of ± 75 ppm ($2\sigma_m$; $n = 14$).

4. Results

Concentrations of Re, Os, Pd, Ir, Pt as well as Os isotopic compositions of chromite from chromite ores from the three mining districts are presented in Table 1, supplemented by corresponding Cr# (Cr/(Cr + Al)) from [27]. Re and Os concentrations vary considerably within each data subset, with Os ranging from 2.6 ppb to 1219 ppb, and Re ranging from 451 ppt to 76.6 ppb. These concentrations are similar to those reported for other ophiolite-hosted chromites ([10], and references therein). As is typical for chromites, the $^{187}Re/^{188}Os$ ratios are generally low, with 19 out of 27 ratios are less than the chondritic average of approximately 0.4. Correspondingly, the age correction was small for most samples. Initial ratios are provided as calculated $^{187}Os/^{188}Os$ ratios, and in the γOs notation, which is the percent deviation of the isotopic composition of a sample from that of the chondritic reference at 90 Ma, the presumed age of formation of the back-arc crust [21,31].

Some of the samples studied herein have previously been analyzed as bulk, unspiked chromitite aliquots [27]. A comparison with the present data set, which is obtained from chromite separates from the same hand specimens, therefore offers a rare opportunity for evaluating the intra-sample Os isotopic variation. Table 1 presents this variation expressed as Δ, which is the percent deviation of the Os isotopic ratio measured on the bulk chromitites from that measured on the chromite separates in this study. Deviations range from −4.4 to +1.3%, but most of the chromite analyses are less radiogenic than those from the bulk chromitites (resulting in negative Δ-values). Our observation of mainly negative Δ-values (Table 1), indicating less radiogenic Os isotopic compositions of chromite separates relative to bulk chromitite sample powders, is consistent with previous experimental results [17], which showed that acid-treated Cr-spinel fractions from abyssal peridotites yield $^{187}Os/^{188}Os$ ratios that are substantially less radiogenic than the corresponding whole rock values. This most likely either reflects the contamination of the "silicate matrix" by radiogenic Os possibly derived by seawater alteration [17], or alteration related to fluid percolation during the tectonic emplacement of the ophiolite [16].

Correlations between initial Os isotopic compositions and chemical parameters, such as Cr# and PGE abundances are shown in Fig. 2A,B,C. Fig. 2A plots the Os concentrations versus γOs values of the studied chromites from the Mayarí–Baracoa ophiolite. In contrast to the study by [27], where Os concentrations of some of the chromitites were analyzed by ICP-MS and INAA on a separate powder aliquot, in this study both Os concentration (via isotope dilution) and Os isotopic composition were analyzed on the same chromite separate. This minimizes the nugget effect and ensures less decoupling of the measured Os isotopic composition

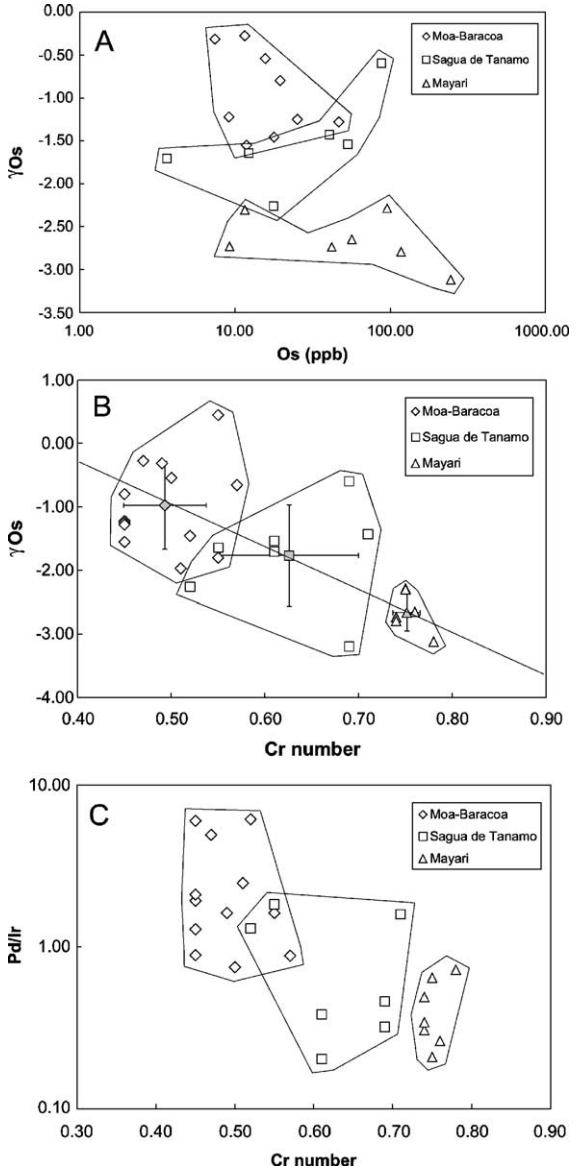

Fig. 2. (A) Diagram showing the relationship between Os concentrations and initial γOs values for chromites from the Mayarí–Baracoa ophiolite belt, grouped into the three mining districts. A weakly defined negative trend is compatible with decreasing degrees of melting, along with progressive arc development of ultramafic rocks associated with the chromites (details in text). (B) Diagram showing the relationship between Cr number and initial γOs values of chromites, grouped according to the three major districts of the Mayarí–Baracoa ophiolite. Grey-filled symbols mark the average composition of each group and the error bars are 1σ. The negatively sloped array reflects the formation of chromites in an evolving magmatic arc setting (see text for details). (C) Diagram showing the relationship between Cr# and Pd/Ir ratio of chromites from the Mayarí–Baracoa ophiolite, grouped into the three major mining districts. The negatively correlated data array reflects the increasing abundance of IPGE relative to PPGE, with increasing degrees of partial melting (reflected by increasing Cr numbers) during the evolution of the arc-related magmas from which the chromites formed (see text for details).

from the measured Os concentration. There is a corresponding weak positive correlation ($R^2=0.3$) between Os concentration and Cr#, when excluding the two samples with the highest concentrations (not shown). The tendency of PGE enrichment with increase in Cr# of the chromite has been observed previously [32–36].

Fig. 2C plots the Pd/Ir ratio versus Cr# of the studied chromites. The negative correlation between the Pd/Ir ratio and the Cr# is similar to that reported by [27], and similar to the γOs versus Cr# correlation in Fig. 2B. This trend is characterized by an increasing enrichment of more compatible PGE (Os, Ir and Ru) with increasing rates of partial melting, indicated by the increasing Cr#. This evolution corresponds to the observed increasingly negative slope of the chondrite-normalized PGE patterns (flat from Os to Ru and negatively sloped from Ru to Pt) of chromitites from the Moa–Baracoa, through the Sagua de Tánamo, to the Mayarí district [27].

5. Discussion

The positive correlation between Os concentration and Cr# (Fig. 2B) and the negative correlation with the Pd/Ir ratio (Fig. 2C) imply that chromite concentrates mainly Os, Ir and Ru, relative to Rh, Pd and Pt (leading to negatively sloped, chondrite-normalized PGE pattern) and suggests a close genetic link between PGE abundances and the nature of the parental melts. PGE and Cr behave compatibly during partial melting as they remain concentrated in residual sulfides and chromian spinel ([37–39]). Melts generated by partial melting of peridotites under relatively dry conditions, like those prevailing at normal mid-ocean ridges and at moderate rates of melting (<25%) become increasingly rich in sulfur, but depleted in PGE. Higher melting rates (>25%), are necessary to remove efficiently the less compatible PGE (Rh, Pt, and Pd) together with sulfides from the residues, but even at such high degrees of melting Os, Ir, and Ru are retained and behave compatibly [39–41]. A combination of high degrees of melting and melt/rock interaction in porous flow channels is necessary to generate Os, Ir and Ru-rich melts like those responsible for the formation of the very Cr-rich chromitites in the Mayarí–Baracoa ophiolite belt [16,42]. Osmium, Ir and Ru behave compatibly during melt percolation processes, even if percolating melts are rich in fluids. It is therefore believed that Al-rich chromites from the mantle–crust transition zone in the Moa–Baracoa and Sague de Tánamo districts formed from PGE-poorer, arc-type melts generated by moderate degrees of melting. In contrast, formation of the Cr-rich chromitites from the

Sagua de Tánamo and Mayarí districts requires PGE-rich melts of boninitic or high-Mg andesite affinity, generated by the percolation of olivine-saturated melts (produced by high degrees of partial melting) through depleted harzburgitic mantle [27].

There is a correlation between the initial $^{187}Os/^{188}Os$ isotopic ratios (expressed in γOs notation) and the Cr# of respective chromites that cluster into three distinct groups representing the mining districts (Table 1, Fig. 2A). Generally the initial $^{187}Os/^{188}Os$ isotopic ratios become lower, i.e. the γOs values become more negative, with increasing Cr#. The average γOs values are: -0.97 ± 0.69 (1σ) for the Moa Baracoa district, -1.77 ± 0.80 (1σ) for the Sagua de Tánamo district and -2.66 ± 0.29 (1σ) for the Mayarí district. These values indicate different Os isotopic evolution paths for the different mantle sections represented by the chromites in the ophiolite. The γOs values are correlated with the chemical composition of the chromites themselves and thus with the degree of partial melting during the formation of the ophiolite. Interestingly, all the chromites from the Mayarí–Baracoa ophiolite belt (with the exception of one sample PO-7; Table 1) are characterized by negative γOs-values. Sample PO-7 contains very high concentrations of Re (76.7 ppb); most likely due to secondary sulfides that are intimately associated with this chromite [19]. Although the $^{187}Re/^{188}Os$ ratio of this sample does not differ from those of the other chromites, the correct in situ correction of the measured $^{187}Os/^{188}Os$ ratio is strongly dependent on the assumption of a closed Re–Os system. A slight Re-loss from sulfides during later alteration processes (weathering) could therefore explain the high initial γOs value, relative to the other values from this district.

The negative γOs values from the Cuba ophiolite are remarkable in comparison with the available literature data on chromites. For example, only 10 out of 55 chromite analyses of a total of 18 Phanerozoic ophiolites distributed across the world with ages ranging from 50 My to 900 My yielded negative γOs values ([10]). The average γOs value obtained in [10] is $+1.31 \pm 1.94$ (1σ). The average γOs value for the 27 samples studied here is -1.62 ± 0.95 (1σ), corresponding to an average initial $^{187}Os/^{188}Os$ ratio of 0.1244 ± 0.0011 (1σ). At the 1σ level, these two averages do not overlap. Instead, the average initial $^{187}Os/^{188}Os$ value defined by the chromites in this study lie within the broad range of 0.120–0.125 proposed by Standish et al. [17] for the upper mantle.

Our observations reveal distinct heterogeneity in initial $^{187}Os/^{188}Os$ ratios, from the scale of the ophiolites to the length scale of individual samples reflecting long-term development with variable Re–Os elemental ratios. This observation is incompatible with the concept of contemporaneous crystallization of PGM from a strictly homogeneous upper mantle and points to the more likely scenario of complex magmatic mechanisms acting upon already existing mantle heterogeneity. It is becoming evident that only large data sets will allow a meaningful, i.e. statistically robust, characterization of the Os isotopic composition of a given upper mantle domain on the length scale of individual ophiolites, as discussed next.

5.1. Mantle evolution models

The Os isotopic composition of the present-day convecting mantle and the exact evolution trajectory of $^{187}Os/^{188}Os$ in the average upper mantle is under debate. Most studies suggest an isotopic evolution similar to, or slightly retarded, relative to the evolution in chondritic meteorites ([10,11,17]). The estimate of 0.1281 for the average present-day upper mantle $^{187}Os/^{188}Os$ ratio deduced from chromite Os isotopic systematics of ophiolites [10] is more radiogenic than previous estimates. A value of 0.1270 was proposed by [43] based on a whole rock data set from a limited number of ophiolites. A value of 0.1246 ± 0.0014 (1σ) was later proposed as an average value of abyssal peridotites by [11]. An average value of 0.124 indicated by a broad distribution of hundreds of PGE alloys from northern California [18]. These relatively low (i.e. 'mantle type') $^{187}Os/^{188}Os$ values have traditionally been considered to be inconsistent with results from modern MORB glasses and sulfide inclusions with $^{187}Os/^{188}Os$ ratios clustering between 0.127 and 0.131; with some samples as high as 0.15 ([44]). Seawater alteration has been invoked to explain this discrepancy between the Os isotopic compositions of peridotites and that of MORB. However, recent in situ observations by [13] in one abyssal peridotite from the Kane fracture zone revealed the presence of different types of magmatic sulfides characterized by $^{187}Os/^{188}Os$ ratios between 0.117 to 0.167, i.e. spanning the entire range previously recorded in abyssal peridotites world wide. None of these sulfides are affected by seawater contamination. Thus, MORB and its source material, abyssal peridotite, are in fact in isotopic equilibrium, but both types of rocks are characterized by substantial Os isotopic heterogeneity.

All in all, the spread in initial Os isotopic ratios of ophiolite-hosted chromites, and of platinum-group minerals from placers which are associated with ophio-

lite and ultramafic intrusions ([18,45–49]) is very large (0.110–0.147) and comparable with that of MORB [13]. Together these observations strongly indicate that the upper mantle is highly heterogeneous in terms of Os isotopic composition at length scales ranging from micrometers to outcrop- and regional length scales.

On this basis, it becomes questionable whether currently available data allows robust conclusions to be reached regarding the average Os isotopic composition of the present-day upper mantle [10]. Our data on chromites of the Mayarí–Baracoa ophiolite distinctly diverge from the time versus initial γOs and $^{187}Os/^{188}Os$ trend determined for ophiolite chromites (Fig. 3). Using the same data as [10] (with omission of the three outliers specified by these authors), together with data for chromites from the 162 Ma Josephine ophiolite [45] and our own data for the Mayarí–Baracoa ophiolite, a linear regression through the average Os isotopic composition from each location yields a present-day intercept at a $^{187}Os/^{188}Os$ ratio of 0.1268 ± 0.0006, which is lower than the value of 0.12808 ± 0.00085 reported by [10], computed as a least squares regression without the data from this study and those from [45]. Thus, a relatively modest addition of new data dramatically changes the estimate for the present-day upper mantle and we therefore consider this exercise to be not very promising, at least on the basis of presently available data from chromites. Only statistically large data sets for each and every ophiolite will provide a meaningful measure of average values and standard deviations for the distributions of Os isotopic heterogeneities that are evidently inherent to the upper mantle at all length scales.

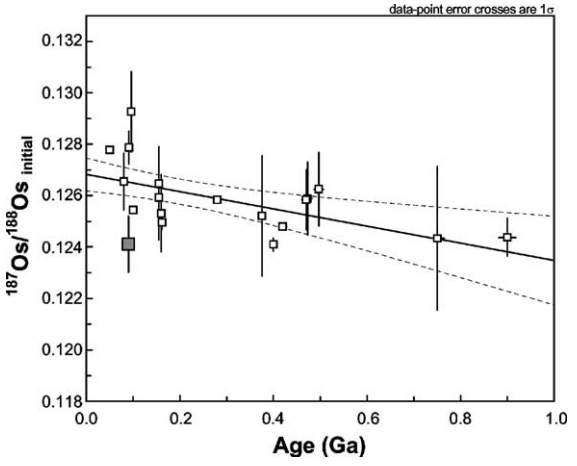

Fig. 3. Time versus initial Os isotopic evolution diagram with average initial $^{187}Os/^{188}Os$ ratios and of Phanerozoic ophiolite-hosted chromites from worldwide locations (empty squares). Averages are computed using data reported by [10] and data from the Josephine ophiolite (northern California) [45]. The average initial $^{187}Os/^{188}Os$ value of the Mayarí–Baracoa ophiolite (computed from 27 chromite analyses listed in Table 1) is plotted with a grey-filled square. Error bars are 1σ. Least square fitting ([52], solid line) of the entire data array results in a present-day (y-intercept) $^{187}Os/^{188}Os$ value of 0.1268 ± 0.0006 (95% confidence, dashed line), which is statistically lower than the value of 0.1281 ± 0.0009 proposed by [10] for the convecting upper mantle.

6. Conclusions

The initial $^{187}Os/^{188}Os$ isotopic ratios of the chromite separates from the Mayarí–Baracoa ophiolite belt in Cuba display distinct regional differences that are correlate with the chemical indicators of their origin; such as Cr#, Os concentration and Pd/Ir ratios. These chemical indicators reflect a progressive change in ophiolite setting, ranging from boninitic (high-Mg) to back-arc basin basaltic affinities in a supra-subduction zone geotectonic environment.

The γOs values from all the districts of the Mayarí–Baracoa ophiolite belt in Cuba are consistently negative, corresponding to an average initial $^{187}Os/^{188}Os$ ratio of 0.1244 ± 0.0012 for the 90 My upper mantle section sampled by of these chromites. Model ages are highly variable and indicate that Re depletion events, some of which took place as far back as 2.1 Ga, are still preserved.

The unradiogenic and variable Os isotopic composition of the chromites from Cuba emphasizes the problem of defining a meaningful average Os isotopic values for the present-day upper mantle, which appears to be highly heterogeneous on all relevant length scales. In combination with data on chromites from the literature, our results show that a "present-day Os isotopic composition" for the upper mantle, the so-called DMM reservoir, cannot be precisely established beyond the statement that it is "broadly chondritic". Instead, our findings are consistent with the "Statistical Upper Mantle Assemblage", or "SUMA"-concept [6], according to which a high level of geochemical heterogeneity is maintained in the upper mantle at all relevant length scales.

Acknowledgments

We thank Toby Leeper for his insightful technical assistance with the mass spectrometer at the Geological Institute. Peter Venslev is thanked for his help in mineral separation. Britta Munch helped with drafting. Two anonymous reviewers provided valuable and critical comments which led to a significant improvement of the manuscript. RF is grateful for financial support through SNF (Statens Naturvidenskabelig Forsknings-

råd; Danish Research Agency) grant number 21-01-0492 56493. This paper is also a contribution to the Spanish research project CGL2004-00622.

References

[1] A.W. Hofmann, Mantle geochemistry: the message from oceanic volcanism, Nature 385 (1997) 219–229.
[2] A. Zindler, S. Hart, Chemical geodynamics, Annu. Rev. Earth Planet. Sci. 14 (1986) 493–571.
[3] C.J. Allègre, D.L. Turcotte, Geodynamic mixing in the mesosphere boundary layer and the origin of oceanic islands, Geophys. Res. Lett. 12 (1985) 207–210.
[4] R.K. Workman, S.R. Hart, M. Jackson, M. Regelous, K.A. Farley, J. Blusztajn, M. Kurz, H. Staudigel, Recycled metasomatized lithosphere as the origin of the enriched mantle II endmember: evidence from the Samoan volcanic chain, Geochem. Geophys. Geosyst. 5 (2004) , doi:10.1029/2003GC000632.
[5] J.C. Lassiter, E.H. Hauri, Osmium-isotope variations in Hawaiian lavas: evidence for recycled oceanic lithosphere in the Hawaiian plume, Earth Planet. Sci. Lett. 164 (1998) 483–496.
[6] A. Meibom, D.L. Anderson, The statistical upper mantle assemblage, Earth Planet. Sci. Lett. 217 (2003) 123–139.
[7] R.G. Coleman, Ophiolites, Springer-Verlag, Heidelberg, 1977, 229 pp.
[8] Y. Dilek, E. Moores, D. Elthon, A. Nicolas, Ophiolites and Oceanic Crust Special Paper, vol. 349, Geological Society of America, Boulder, 2000.
[9] L. Reisberg, A. Zindler, Extreme isotopic variations in the upper mantle; evidence from Ronda, Earth Planet. Sci. Lett. 81 (1986) 29–45.
[10] R.J. Walker, H.M. Prichard, A. Ishiwatari, M. Pimentel, The osmium isotopic composition of convecting upper mantle deduced from ophiolite chromites, Geochim. Cosmochim. Acta 66 (2002) 329–345.
[11] J.E. Snow, L. Reisberg, Os isotopic systematics of the MORB mantle; results from altered abyssal peridotites, Earth Planet. Sci. Lett. 133 (1995) 411–421.
[12] B.M. Roy, G.J. Wasserburg, D.A. Papanastassiou, M. Chaussidon, Osmium isotopic compositions and Re–Os concentrations in sulfide globules from basaltic glasses, Earth Planet. Sci. Lett. 154 (1998) 331–347.
[13] O. Alard, A. Luguet, N.J. Pearson, W.L. Griffin, J.-P. Lorand, A. Gannoun, K.W. Burton, S.Y. O'Reilly, In situ Os isotopes in abyssal peridotites bridge the isotopic gap between MORBs and their source mantle, Nature 436 (2005) 1005–1008.
[14] A. Tsuru, R.J. Walker, A. Kontinen, P. Peltonen, E. Hanski, Re–Os isotopic systematics of the 1.95 Ga Jormua ophiolite complex, northeastern Finland, Chem. Geol. 164 (2000) 123–141.
[15] R. Frei, B.K. Jensen, Re–Os, Sm–Nd isotope- and REE systematics on ultramafic rocks and pillow basalts from the Earth's oldest oceanic crustal fragments (Isua supracrustal belt and Ujaragssuit nunat area, W Greenland), Chem. Geol. 196 (2003) 163–191.
[16] A. Büchl, G. Bruegmann, V.G. Batanova, C. Muenker, A.W. Hofmann, Melt percolation monitored by Os isotopes and HSE abundances; a case study from the mantle section of the Troodos Ophiolite, Earth Planet. Sci. Lett. 204 (2002) 385–402.
[17] J.J. Standish, J. Hart, J. Blusztajn, H.J.B. Dick, K.L. Lee, Abyssal peridotite osmium isotopic compositions from Cr-spinel, Geochem. Geophys. Geosyst. (2002) GC000161.
[18] A. Meibom, N.H. Sleep, C.P. Chamberlain, R.G. Coleman, R. Frei, M.T. Hren, J.L. Wooden, Re–Os isotopic evidence for long-lived heterogeneity and equilibration processes in the Earth's upper mantle, Nature 419 (2002) 705–708.
[19] O. Alard, W.L. Griffin, J.P. Lorand, S.E. Jackson, Non-chondritic distribution of the highly siderophile elements in mantle sulphides, Nature 407 (2000) 891–894.
[20] E.H. Hauri, S.R. Hart, Rhenium abundances and systematics in oceanic basalts, Chem. Geol. 139 (1997) 185–205.
[21] M. Iturralde-Vinent, Cuban geology: a new plate tectonic synthesis, J. Pet. Geol. 17 (1994) 30–70.
[22] J. Proenza, F. Gervilla, J. Melgarejo, J.L. Bodinier, Al- and Cr-rich chromitites from the Mayari–Baracoa ophiolitic belt (eastern Cuba); consequence of interaction between volatile-rich melts and peridotites in suprasubduction mantle, Econ. Geol. 94 (1999) 547–566.
[23] C. Marchesi, C.J. Garrido, J.A. Proenza, M. Godard, F. Gervilla, R. Diaz-Martínez, New geochemical data on peridotites from Mayari–Cristal and Moa–Baracoa ophiolitic massifs (eastern Cuba), New geochemical data on peridotites from Mayari–Cristal and Moa–Baracoa ophiolitic massifs (eastern Cuba), 32nd IGC, 1994, pp. 214–216.
[24] V.I. Murashako, R.M. Lavandero, Chromite in the hyperbasite belt of Cuba, Int. Geol. Rev. 31 (1989) 90–99.
[25] J.A. Proenza, F. Gervilla, J.C. Melgarejo, O. Vera, P. Alfonso, A.E. Fallick, Genesis of sulfide-rich chromite ores by the interaction between chromitite and pegmatitic olivine-norite dikes in the Potosi Mine (Moa–Baracoa ophiolitic massif, eastern Cuba), Miner. Depos. 36 (2001) 658–669.
[26] J.A. Proenza, J.C. Melgarejo, F. Gervilla, A. Rodríguez-Vega, R. Diaz-Martínez, R. Ruiz-Sánchez, W. Lavaut, Coexistence of Cr- and Al-rich ophiolitic chromitites in a small area: the Sague de Tanamo district, Eastern Cuba, in: Eliopoulos (Ed.), Mineral Exploration and Sustainable Development, Millpress, Rotterdam, 2003, pp. 631–634.
[27] F. Gervilla, J.A. Proenza, R. Frei, C.J. Garrido, J.C. Melgarejo, A. Meibom, R. Diaz-Martinez, W. Lavaut, Distribution of platinum-group elements and Os isotopes in chromite ores from Mayari–Baracoa Ophiloitic Belt (eastern Cuba), Contrib. Mineral. Petrol. 150 (2005) 589–607.
[28] T.F. Nägler, R. Frei, Plug in plug osmium distillation, Schweiz. Mineral. Petrogr. Mitt. 76 (1997) 123–127.
[29] J.L. Birck, M.R. Barman, F. Capmas, Re–Os isotopic measurements at the femtomole level in natural samples, Geostand. Newsl. 21 (1997) 19–27.
[30] A.S. Cohen, F.G. Waters, Separation of osmium from geological materials by solvent extraction for analysis by thermal ionisation mass spectrometry, Anal. Chim. Acta 332 (1996) 269–275.
[31] M.A. Iturralde-Vinent, C. Diaz Otero, A. Rodríguez-Vega, R. Diaz-Martínez, Tectonic implications of paleontologic dating of Cretaceous-Danian sections of Northeastern Cuba, Geologica Acta (in press).
[32] J.H. Crocket, Platinum-group elements in mafic and ultramafic rocks, a survey, Can. Mineral. 17 (1979) 391–402.
[33] M.I. Economou, Platinum group elements (PGE) in chromite and sulphide ores within the ultramafic zone of some Greek ophiolite complexes, in: M.J. Gallagher, R.A. Ixer, C.R. Neary, H.M. Prichard (Eds.), Metallogeny of Basic and Ultrabasic Rocks, 1986, pp. 441–453.
[34] M. Leblanc, G. Ceuleneer, Chromite crystallization in a multicellular magma flow; evidence from a chromitite dike in the Oman Ophiolite, Lithos 27 (1991) 231–247.

[35] M. Leblanc, Chromitite and ultramafic rock compositional zoning through a paleotransform fault, Poum, New Caledonia, Econ. Geol. 90 (1995) 2028–2039.
[36] A.H. Ahmed, S. Arai, Unexpectedly high-PGE chromitite from the deeper mantle section of the northern Oman Ophiolite and its tectonic implications, Contrib. Mineral. Petrol. 143 (2002) 263–278.
[37] R.H. Mitchell, R.R. Keays, Abundance and distribution of gold, palladium and iridium in some spinel and garnet lherzolites; implications for the nature and origin of precious metal-rich intergranular components in the upper mantle, Geochim. Cosmochim. Acta 45 (1981) 2425–2442.
[38] S.J. Barnes, B.R.A. Korneliussen, L.P. Nilsson, M. Often, R.B. Pedersen, B. Robins, The use of mantle normalization and metal ratios in discriminating between the effects of partial melting, crystal fractionation and sulfide segregation on platinum-group elements, gold, nickel and copper: examples from Norway, in: H.M. Prichard, P.J. Potts, J.F.W. Bowles, S.J. Cribb (Eds.), Geoplatinum, vol. 87, Elsevier, London, 1988, pp. 113–144.
[39] J.P. Lorand, L. Pattou, M. Gros, Fractionation of platinum-group elements and gold in the upper mantle; a detailed study in Pyrenean orogenic lherzolites, J. Petrol. 40 (1999) 957–981.
[40] G.E. Brügmann, N.T. Arndt, A.W. Hofmann, H.J. Tobschall, Noble metal abundances in komatiite suites from Alexo, Ontario, and Gorgona Island, Colombia, Geochim. Cosmochim. Acta 51 (1987) 2159–2169.
[41] C. Bockrath, C. Ballhaus, A. Holzheid, Fractionation of the platinum-group elements during mantle melting, Science 305 (2004) 1951–1953.
[42] A. Büchl, G.E. Brügmann, V.G. Batanova, A.W. Hofmann, Os mobilization during melt percolation: the evolution of Os isotopic heterogeneities in the mantle sequence of the Troodos ophiolite, Cyprus, Geochim. Cosmochim. Acta 68 (2004) 3397–3408.
[43] J.M. Luck, C.J. Allègre, Osmium isotopes in ophiolites, Earth Planet. Sci. Lett. 107 (1991) 406–415.
[44] M. Roy-Barman, C.J. Allègre, $^{187}Os/^{186}Os$ ratios of mid-ocean ridge basalts and abyssal peridotites, Geochim. Cosmochim. Acta 58 (1994) 5043–5054.
[45] R. Walker, A.D. Brandon, J.M. Bird, P.M. Piccoli, W.F. McDonough, R.D. Ash, ^{187}Os-^{186}Os systematics of Os-Ir-Ru alloy grains from southwestern Oregon, Earth Planet. Sci. Lett. 230 (2005) 211–226.
[46] A. Meibom, R. Frei, Evidence for an ancient osmium isotopic reservoir in Earth, Science 296 (2002) 516–519.
[47] A. Meibom, R. Frei, N.H. Sleep, Osmium isotopic compositions of Os-rich platinum group element alloys from the Klamath and Siskiyou mountains, J. Geophys. Res. 109 (2004) B02203.
[48] K. Hattori, S.R. Hart, Osmium isotope ratios of PGM-minerals from alpine-type ultramafic rocks and associated placers, in: Anonymous (Ed.), AGU 1990 fall meeting, 1990, pp. 1713–1714.
[49] K. Hattori, S.R. Hart, Osmium-isotope ratios of platinum-group minerals associated with ultramafic intrusions—Os-isotopic evolution of the oceanic mantle, Earth Planet. Sci. Lett. 107 (1991) 499–514.
[50] S.B. Shirey, R.J. Walker, The Re–Os isotope system in cosmochemistry and high-temperature geochemistry, Annu. Rev. Earth Planet. Sci. 26 (1998) 423–500.
[51] M.I. Smoliar, R.J. Walker, J.W. Morgan, Re–Os ages of Group IIA, IIIA, IVA, and IVB iron meteorites, Science 271 (1996) 1099–1102.
[52] K. Ludwig, Isoplot/Ex, Version 2.01b, A geochronological toolkit for Microsoft Excel, Berkely Geochronological Center Special Publication, vol. 1a, 1999 (43 pp.).